High-pressure BaCrO3 polytypes and the 5H–BaCrO2.8 phase

High-pressure $BaCrO_3$ polytypes and the 5H-$BaCrO_{2.8}$ phase

*Angel M. Arévalo-López and J. Paul Attfield **

Centre for Science at Extreme Conditions (CSEC) and School of Chemistry, University of Edinburgh, Mayfield Road, Edinburgh EH9 3FD (UK)

Abstract

Polytypism of $BaCrO_3$ perovskites has been investigated at 900-1100 °C and pressures up to 22 GPa. Hexagonal 5H, 4H, and 6H perovskites are observed with increasing pressure, and the cubic 3C perovskite (a = 3.99503(1) Å) is observed in bulk form for the first time at 19-22 GPa. An oxygen-deficient material with limiting composition 5H-$BaCrO_{2.8}$ is synthesised at 1200 °C under ambient pressure. This contains double tetrahedral Cr^{4+} layers and orders antiferromagnetically below 260 K with a (0 0 1/2) magnetic structure.

1. Introduction

Chromium-based perovskite oxides are important mixed conductors in solid-oxide fuel cells (SOFC) anodes where materials such as $(La_{1-x}Sr_x)(Cr_{1-y}M_y)O_{3-\delta}$ (M = Mn, Fe, Co, Ni) [1] show high ionic conductivities due to oxide vacancies and electronic conductivities arising from variable cation oxidation states. Other materials have very high magnetic ordering transition temperatures such as in the ferrimagnetic double perovskite Sr_2CrOsO_6 with an ordering temperature of 725 K, [2] and even cation-disordered analogues $Sr(Cr_{1-x}Ru_x)O_3$ ($0.4 < x < 0.6$) have transitions at 410-480 K. [3,4]

New Cr-based perovskite vacancy superstructure phases have recently been synthesised using hard-soft chemistry, where $ACrO_3$ (A = Ca, Sr) [5] perovskites prepared under "hard" high pressure and temperature conditions were subsequently reduced using "soft" low temperature hydrogen or hydride reagents. Reduction of cubic $SrCrO_3$ gave new $SrCrO_{2.8}$ and $SrCrO_{2.75}$ products. [6] $SrCrO_{2.8}$ was discovered to have a 15R (15-layer rhombohedral) superstructure with an all cubic $(ccc'cc)_3$ stacking sequence reminescent of long period hexagonal perovskites based on mixed cubic (c) and hexagonal (h) stacking sequences. Rearrangement of oxides in the c' oxygen-deficient layer changes the coordination around Cr^{4+} from octahedral to tetrahedral which is generally more stable at ambient prerssure. The 15R-$SrCrO_{2.8}$ type superstructure has subsequently been stabilised in $SrCr_{1-x}Fe_xO_{3-y}$ perovskites ($0.4 \leq x \leq 0.6$) without requiring hard-soft synthesis.[7] These are ferrimagnetic with ordering temperatures of 225-340 K. The perovskite $SrCrO_3$ and the reduced $SrCrO_{2.8}$ structure were also stabilised epitaxially as thin films,

with rapid oxygen uptake or loss on cycling between the two phases.[8] The hard-soft route was also used to discover three new reduced $CaCrO_{3-\delta}$ (δ = 0.33, 0.4 and 0.5) phases.[9] The most reduced phase, $Ca_2Cr_2O_5$, is an unusual Cr^{3+} brownmillerite structure with antiferromagnetic order at 220 K and a substantial canting of ordered moments.[10]

The above $ACrO_3$ (A = Ca, Sr) precursor perovskites are only formed in a cubic-type (3C) polytype at moderate pressures, but a variety of hexagonal perovskite polytypes are known for the A = Ba analogue. Early investigations by Chamberland and co-workers at pressures of 6.0-6.5 GPa reported 4H, 6H, 9R, 27R and 14H polytypes as a function of starting materials, temperature and heating time.[11,12,13,14,15] An oxygen deficient $BaCrO_{2.9}$ 5H polytype was also synthesized without the use of high pressure.[16] The cubic 3C form was recently grown as a film on a lattice matched substrate using pulsed laser deposition,[17] but has not been reported as a bulk phase.

Here we report an investigation of the $BaCrO_3$ P-T phase diagram, including stabilisation of the 3C phase in bulk for the first time and also a study of the structure and oxygen content of the 5H polytype. The crystal structure and discovered ferrimagnetic properties of the 6H-$BaCrO_3$ polytype which has a Curie transition at T_C = 192 K were recently reported elsewhere.[18]

2. Experimental

5H-$BaCrO_{3-\delta}$ was synthesised at ambient pressure following the method outlined in the literature [16]; a 2:1 ratio of $BaCO_3$ and Cr_2O_3 was ground, pelleted and fired in a tube furnace at 1200 ºC under flowing argon. Attempts to perform this reaction at temperatures of 1100 °C and below resulted in a mixture of $Ba_3Cr_2O_8$ and Cr_2O_3.

High pressure syntheses used a 2:1 mixture of $Ba_3Cr_2O_8$ and Cr_2O_3. $Ba_3Cr_2O_8$ was used to provide excess oxygen pressure to stabilise Cr^{4+}, and to avoid introducing carbonate or hydroxide into the high pressure reactions, as these species may have been present in the BaO used for some syntheses by Chamberland [11]. Polycrystalline $Ba_3Cr_2O_8$ was prepared by heating a pellet of $BaCO_3$ and Cr_2O_3 in a 3:1 ratio at 1100 ºC in a tube furnace under flowing Ar gas followed by quenching into liquid nitrogen. High pressure syntheses were carried out using a two-stage Walker-type press. Samples were compressed under pressures up to 22 GPa, heated in 15 min up to reaction temperatures of 900-1100 ºC, held at the reaction temperature 30 min, rapidly cooled to ambient temperature, and finally decompressed. A 14/8 sample configuration was used for pressures up to 11 GPa, and 5/3 was used for higher pressures.

Laboratory powder x-ray diffraction profiles from flat-plate samples were recorded on a Bruker D2 instrument using Cu-K_α radiation. Synchrotron x-ray diffraction data from samples in a glass capillary were obtained at the I11 beamline of the Diamond Light Source with wavelength 0.824759 Å. Time-of-flight neutron diffraction data were collected from a 1.9 g sample of 5H-$BaCrO_{2.8}$ between 5 and 300 K using the GEM diffractometer at the ISIS facility.

Thermogravimetric analysis (TGA) data of 5H-$BaCrO_{3-\delta}$ samples were measured under flowing oxygen up to 800 ºC in a Netzch STA 449 F1 Jupiter apparatus. Magnetisation data were measured on a Quantum Design MPMS SQUID magnetometer. Susceptibilities in zero field cooled (ZFC) and field cooled (FC) conditions were recorded in the 2-300 K temperature range with a 5000 Oe applied field.

3. Results and Discussion

3.1 $BaCrO_3$ Polytypes

With increasing pressure, 5H, 4H, 6H and 3C (the arisotype cubic) perovskites were observed. Our results are broadly consistent with those of Chamberland [11] where 4H and 6H phases were observed at 6.0-6.5 GPa and temperatures of 750-1200 °C. We did not explore the 1200-1300 °C region where more complex 14H and 27R polytypes were crystallised at pressure.[12,14] Indexed powder x-ray diffraction patterns of the observed $BaCrO_3$ polytypes are shown in Figure 1(a) and an approximate P-T phase diagram summarising our synthesis results is displayed in Figure 1(b). Rietveld fits are shown as Supplementary Material.

The simple cubic aristotype 3C-$BaCrO_3$ perovskite structure was recently stabilised epitaxially as a film on a $SrTiO_3$ substrate,[17] but the bulk material has not previously been reported. We have found that 3C perovskite can be recovered from syntheses at pressures above ~20 GPa although single phase samples were not obtained (see Figs. 1(a) and 2). One of the secondary phases was a new pseudo-hollandite type which we have assigned and fitted as $Ba_{1.8}Cr_6O_{12}$ (space group $P6_3/m$, a = 9.1707(1) Å, c = 2.8529(1) Å).

Layer stacking sequences and the cell parameters for the different polytypes are summarized in Table 1. The proportion of cubic stacking generally increases with pressure as found in other polytypic perovskite systems although the stability of the lowest pressure 5H structure, described in the next section, with 60% c layers appears anomalous. The cell volume per $BaCrO_{3-\delta}$ formula unit (V/Z) decreases with increasing synthesis pressure, except for the 3C phase which has an anomalously large volume in comparison to the 6H phase. This suggests that there may be some oxygen-deficiency in the cubic phase, which reduces the perovskite tolerance factor from the relatively high value of t = 1.09 predicted for 3C-$BaCrO_3$. A similar stabilisation of cubic $BaCoO_{3-\delta}$ with a large δ = 0.8 deficiency was recently reported. [19]

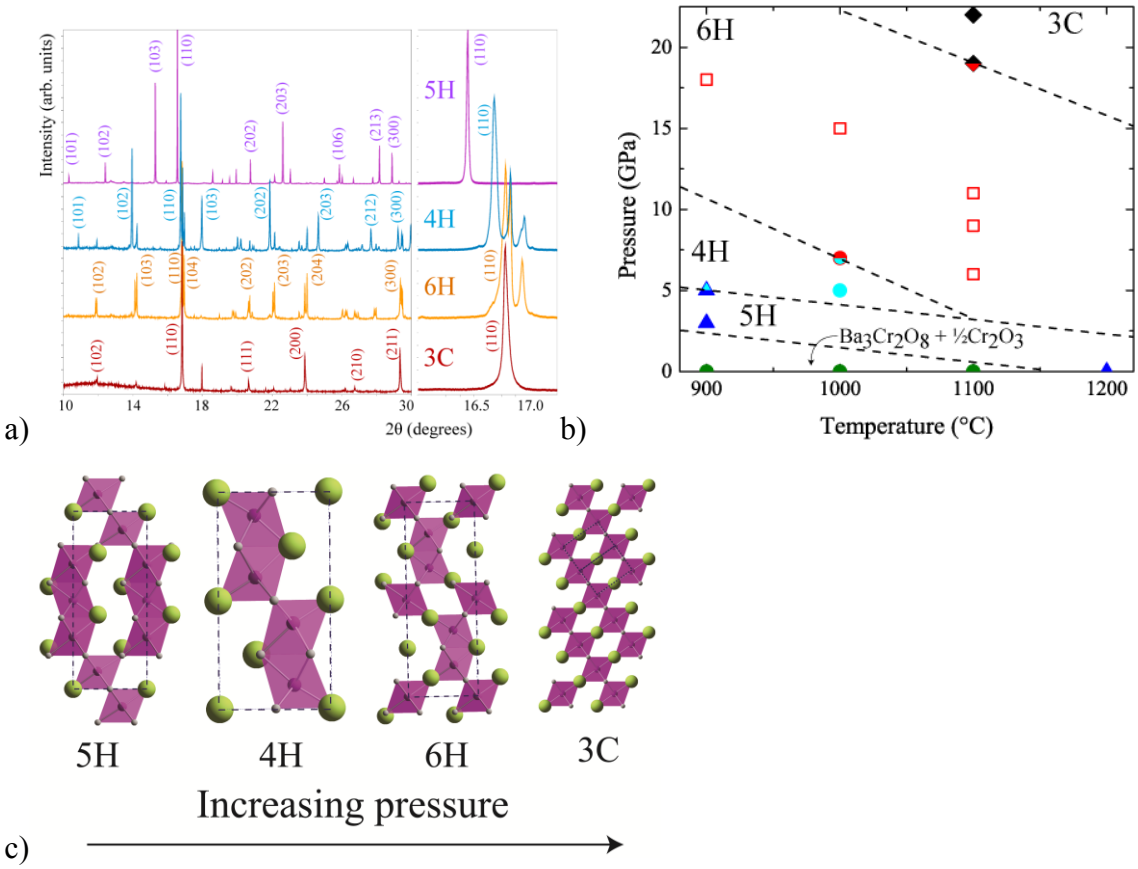

Figure 1. (a) Indexed powder X-ray diffraction data for $BaCrO_3$ polytypes prepared with pressure/temperature/heating time as shown; 5H – 3 GPa/900 ºC/ 30 min; 4H – 5 GPa/1000 ºC/ 30 min; 6H – 9 GPa/1100 ºC/ 30 min; 3C – 22 GPa/1100 ºC/ 30 min. (b) An approximate P-T phase diagram for $BaCrO_3$ showing the results of the present study. (c) Crystal structures of the observed $BaCrO_3$ polytypes showing changes in stacking sequences with pressure. Ba/Cr/O are shown as large/medium/small spheres.

Table 1. Stacking sequences and space groups for $BaCrO_{3(-\delta)}$ polytypes and refined room temperature cell parameters and volume per formula unit using synchrotron powder x-ray data unless indicated.

Polytype	Stacking sequence	Space group	*a* (Å)	*c* (Å)	*V*/*Z* (Å^3)
5H ($\delta = 0$)[a]	*hccch*	*P-3m1*	5.7290(4)	11.9123(3)	67.72
5H ($\delta = 0.2$)	*hcc'ch*	*P-3m1*	5.7305(2)	11.9175(1)	67.78
4H	*hchc*	*P6$_3$/mmc*	5.66597(4)	9.4120(1)	65.42
6H	*chcchc*	*P6$_3$/mmc*	5.62839(7)	13.6773(2)	62.54
3C	*ccc*	*Pm-3m*	3.99503(1)	–	63.76

[a] From laboratory Cu-K$_\alpha$ radiation.

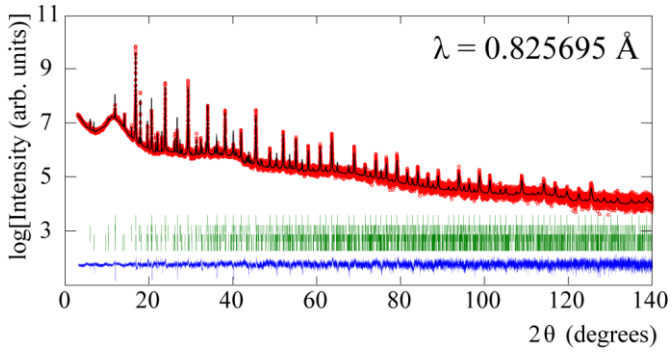

Figure 2. Rietveld fit to 300 K synchrotron powder x-ray data for a 3C-$BaCrO_3$ sample prepared at 22 GPa. Upper/middle/lower reflection markers correspond to 3C-$BaCrO_3$ (60 weight %), the new pseudo-hollandite phase $Ba_{1.8}Cr_6O_{12}$ (13 %) and 6H-$BaCrO_3$ (27 %) respectively. Intensity is plotted on a log scale to show the secondary contributions. Refinement results for 3C-$BaCrO_3$ in space group *Pm-3m*; a = 3.99503(1) Å; overall isotropic B-factor = 0.271(7) $Å^2$; residuals R_{wp} = 0.091 and R_p = 0.062.

The $BaCrO_{3-\delta}$ system shows strong similarities to $BaVO_{3-\delta}$, where hexagonal 12R and 14H polytypes were obtained at 6 GPa and 1200 °C [20] and 3C-$BaVO_3$ is stabilised at pressures above 15 GPa and 1350 °C.[21] There is also an analogous reduction behaviour between the 5H polytypes of $BaCrO_{3-\delta}$ and $BaVO_{3-\delta}$, as described in the next section.

3.2 5H-$BaCrO_{3-\delta}$ phases

Following an earlier report [16] we found that an oxygen deficient 5H-$BaCrO_{3-\delta}$ phase with $\delta \approx 0.2$ can be synthesised at 1200 °C under ambient pressure conditions, although a mixture of $Ba_3Cr_2O_8$ and Cr_2O_3 was obtained using temperatures below 1100 °C. However, application of 3 GPa pressure stabilises the 5H phase at 900 °C. The oxygen content of 5H-$BaCrO_{3-\delta}$ was investigated at ambient pressure and a range $0 \leq \delta \leq 0.2$ was found. The $\delta = 0$ phase was prepared by oxidising pristine material synthesised at 1200 °C and ambient pressure for 12 hrs in air at 350 ºC, and $\delta = 0.2$ was obtained by heating under flowing hydrogen at 350 ºC for 12 hrs. The oxygen contents of these two limiting compositions were confirmed by oxidative TGA as shown in Figure 3. The same range of oxygen contents was reported in the vanadium analogue system 5H-$BaVO_{3-\delta}$ [22] and the structural relationship is confirmed by our neutron diffraction results shown later.

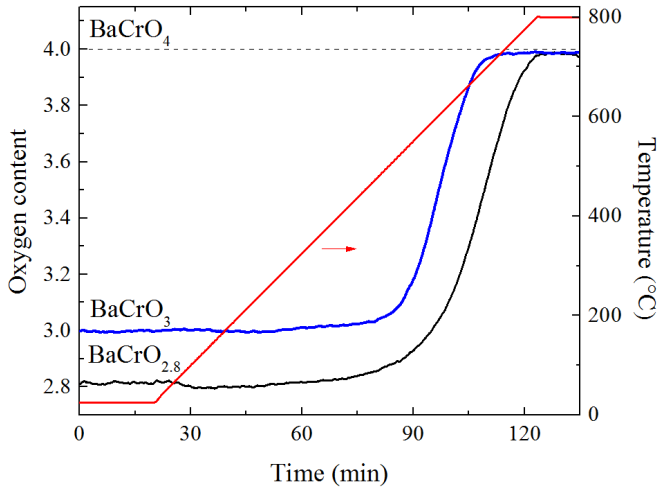

Figure 3. Thermogravimetric analysis of two 5H-$BaCrO_{3-\delta}$ samples confirming their limiting $\delta = 0$ and $\delta = 0.2$ compositions. Samples were heated under flowing oxygen gas with the temperature profile shown. Oxygen contents from weight changes are normalised to the $BaCrO_4$ product.

Magnetic susceptibility measurements on 5H-$BaCrO_{2.8}$ in Fig. 3 reveal a sharp magnetic Néel transition at $T_N = 250$ K. Below 48 K, ZFC and FC data diverge due to the presence of $BaCr_2O_4$ secondary phase. Although our measurements up to 300 K do not cover a sufficient temperature range for reliable Curie-Weiss fitting, a fit in the $260 < T < 300$ K region gives indicative values of 3.4 μ_B for the paramagnetic moment and -684 K for the Weiss temperature. The former value is between the ideal values of 2.83 μ_B and 3.87 μ_B for localised S = 1 (Cr^{4+}) and 3/2 (Cr^{3+}) spins respectively. The large negative Weiss temperature shows that antiferromagnetic spin-spin interactions are dominant.

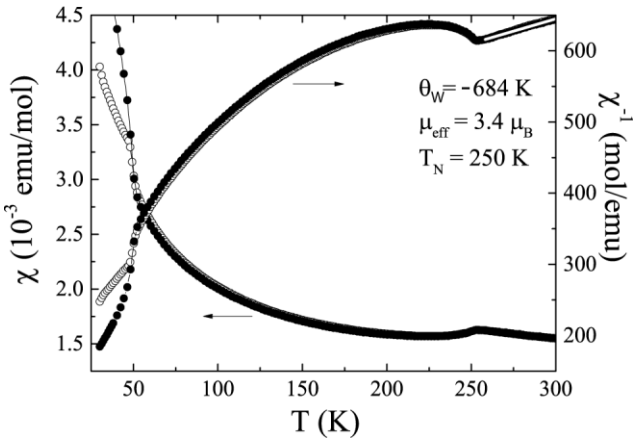

Figure 3. ZFC and FC magnetic susceptibilities for 5H-$BaCrO_{2.8}$ and the inverse susceptibilities showing a Curie-Weiss fit above 260 K. The transition at 48 K corresponds to the $BaCr_2O_4$ secondary phase.

Neutron diffraction data were collected from a 1.9 g 5H-$BaCrO_{2.8}$ sample, synthesised at 1200 °C and ambient pressure, on the GEM diffractometer at the ISIS facility. The nuclear data were fitted well by the model reported for 5H-$BaVO_{2.8}$ [21] and 5H-$BaCoO_{2.8}$ [23] with Cr at V/Co positions and oxygen 2*d* sites in the z = 0 plane fully occupied while alternative 3*e* sites are empty, occupation of the 3*e* sites gives the ideal 5H-$BaCrO_3$ structure shown in Fig. 1c. The structure consists of three layers of face-sharing CrO_6 octahedra and two layers of CrO_4 tetrahedra as shown in Figure 4. The contribution from 13% wt of the secondary phase $BaCr_2O_4$ was also fitted. Results of the refinement at 280 K are summarized in Tables 2 and 3.

Reduction of 5H-$BaCrO_3$ to 5H-$BaCrO_{2.8}$ (and the same for V analogues [21]) results in the loss of one oxygen from the z = 0 plane while the remaining two undergo a rearrangement becoming coordinated to one Cr each and thus creating tetrahedral environments in the two adjacent Cr layers. Bond valence sum (BVS) [24] estimates of Cr oxidation states using bond distances in Table 2 and a standard interpolation formula [25] are Cr1 = 3.9, Cr2 = 2.9 and Cr3 = 3.4. Taking the tetrahedral Cr1 site to be Cr^{4+} gives renormalised valences for the octahedral Cr2 and Cr3 sites as 3.15 and 3.7, showing that they are respectively close to Cr^{3+} and Cr^{4+} states although perhaps with some charge transfer between sites.

Long range spin order in 5H-$BaCrO_{2.8}$ is confirmed by the appearance of magnetic neutron diffraction peaks below 250 K (Figure 4). Their intensities are fitted by a simple model with propagation vector (0 0 1/2) where Cr spins in every layer are parallel, and each ferromagnetic layer is antiferromagnetically coupled to adjacent spin-planes leading to the doubled *c*-axis periodicity. Magnetic moments are parallel to the c-axis with refined magnitudes of 1.4(2), 2.1(1) and 0.9(1) μ_B for Cr1, Cr2 and Cr3 moments at 5 K. Their relative magnitudes are consistent with the assigned oxidation states of +4, +3 and +4 respectively, allowing for reductions from the ideal values of 2 μ_B for S = 2 Cr^{4+} and 3 μ_B for S = 3/2 Cr^{3+} due to zero-point, covalency, and perhaps frustration effects. The three moments show similar critical variations with a fitted transition temperature of T_N = 263.3(1) K and critical exponent β = 0.27, as shown in Figure 4(b).

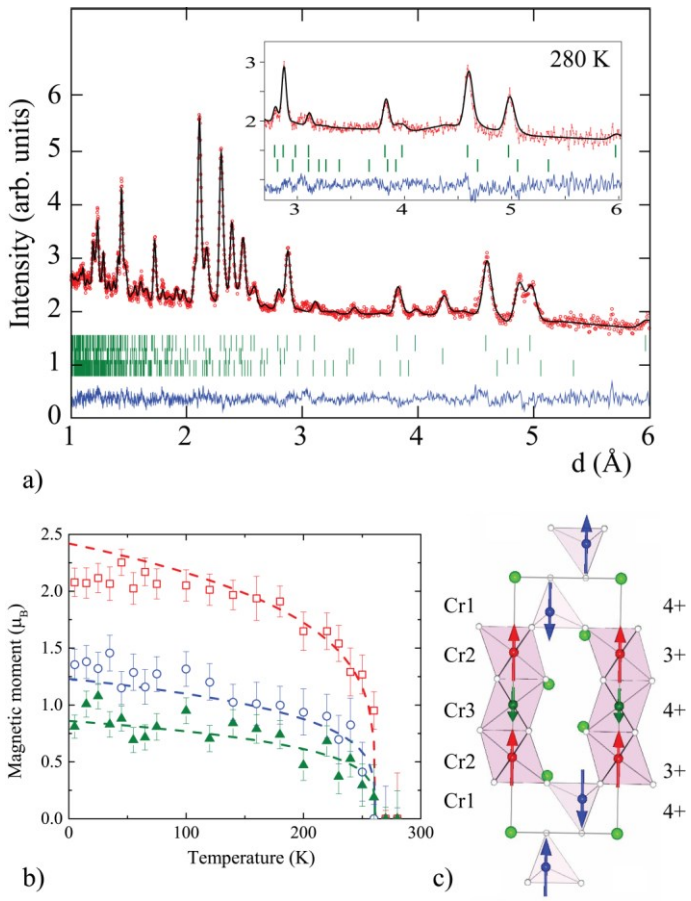

Figure 4. (a) Rietveld fit to neutron diffraction data for 5H-$BaCrO_{2.8}$ collected at 5 K (upper, middle and lower reflection markers respectively correspond to the crystal structure, the magnetic structure and the secondary phase $BaCr_2O_4$). Inset shows the long-*d* region of 280 K data where no magnetic peaks are present for comparison. (b) Temperature variations of the refined magnetic moments for the three distinct Cr sites, coloured as shown in (c) and fitted with $(1\text{-}T/T_N)^{\beta}$ where T_N = 263.3(1) K and β = 0.27. (c) Crystal and magnetic structures showing the distinct Cr sites and the assigned oxidation states.

Table 2. Refined parameters for 5H-$BaCrO_{2.8}$ in space group *P-3m1* from the fit to 280 K neutron powder diffraction data.[a]

Atom	Site	*x*	*y*	*z*	B_{iso} (Å^2)
Ba1	1*a*	0	0	0	0.76(2)
Ba2	2*d*	⅓	⅔	0.7709(10)	0.76
Ba3	2*d*	⅓	⅔	0.4218(9)	0.76
Cr1	2*d*	⅓	⅔	0.1322(10)	0.43(2)
Cr2	2*c*	0	0	0.2933(12)	0.43
Cr3	1*b*	0	0	½	0.43
O1	2*d*	⅓	⅔	0	0.76(1)
O2	6*i*	0.1667(9)	-0.1667	0.1932(4)	0.76
O3	6*i*	0.1513(6)	-0.1513	0.6022(6)	0.76

[a] Cell parameters a = 5.7319(2) and c = 11.9183(6) Å. Residuals R_{wp} = 0.028 and R_p = 0.023.

Table 3. Selected bond distances (Å), angles (°) for the Cr sites in 5H-$BaCrO_{2.8}$ from refinement against 280 K neutron diffraction data.

Cr1−O1 x1	1.57(1)
Cr1−O2 x3	1.81(1)
Cr2−O2 x3	2.04(1)
Cr2−O3 x3	1.95(1)
Cr3−O3 x6	1.93(1)
O1-Cr1-O2 x3	113.7(6)
O2-Cr1-O1 x3	104.9(5)
O2-Cr2-O2 x3	89.3(5)
O2-Cr2-O3 x6	93.5(5)
O2-Cr2-O3 x3	176.1(6)
O3-Cr3-O3 x6	84.5(3)
O3-Cr3-O3 x3	180

It is notable that the structural mechanism for oxygen loss and rearrangement during the reduction of 5H-$BaMO_3$ to 5H-$BaMO_{2.8}$ (M = Cr, V) is the same as for the reduction of the cubic high pressure perovskite $SrCrO_3$ to 15R-$SrCrO_{2.8}$ [6]. The rearrangement creates a double layer of tetrahedra containing

M^{4+} ions while some cations in the remaining octahedral layers are reduced to the M^{3+} state to maintain charge neutrality. The structural requirement for this mechanism is the presence of a …*cc'c*… sequence within the stacked layers, where *c*' represents the rearranged, oxygen-deficient AO_2 (A = Sr or Ba) layer. This avoids bringing the tetrahedrally coordinated cations into close contact with each other, or with octahedral cations in the adjacent layers. The same mechanism was reported for 12H-$BaCoO_{2.61}$ which has the $(hcc'chh)_2$ stacking sequence and additional random oxygen vacancies.[26] 5H-$BaCrO_{2.8}$ has a 5-layer (*hcc'ch*) sequence imposed by the packing in the 5H-$BaCrO_3$ precursor, whereas 15R-$SrCrO_{2.8}$ spontaneously forms a triple five-layer $(ccc'cc)_3$ sequence with all layers being cubically packed.

The 5H-$BaMO_{2.8}$ and 15R-$SrCrO_{2.8}$ systems differ in the charge distributions within the tetrahedral (T) and octahedral (O) cations. These are $Cr^{4+}{}_TCr^{3+}{}_OCr^{4+}{}_OCr^{3+}{}_OCr^{4+}{}_T$ in 5H-$BaCrO_{2.8}$ but $Cr^{4+}{}_TCr^{3.5+}{}_OCr^{3+}{}_OCr^{3.5+}{}_OCr^{4+}{}_T$ in 15R-$SrCrO_{2.8}$. Both distributions may be described as charge density waves pinned by the *c'* layers, and they give rise to (0 0 1/2) spin density waves in both materials where layers of spins are antiferromagnetically coupled to their neighbours and the magnitudes of ordered moments follow the formal oxidation states.

An unusual feature of the 5H-$BaMO_{2.8}$ and 15R-$SrCrO_{2.8}$ structures compared to reduced perovskites in general is that the oxygen vacancies are highly segregated, with one third of the oxides missing from every fifth close-packed *c'* layer while the other four layers are pristine. This local concentration of vacancies within the reconstructed layers may facilitate oxide ion migration and *c'*-like defect regions may be responsible for the high oxide ion conductivity associated with doped Cr-perovskites used as solid oxide fuel cell (SOFC) anodes. [27]

4. Conclusions

This study confirms that several $BaCrO_3$ polytypes can be synthesised at high pressures and temperatures. 4H, 5H, and 6H polytypes are observed at 900-1100 °C and pressures up to 20 GPa, and the cubic 3C perovskite phase is observed at 19-22 GPa. An oxygen-deficient form of the 5H polytype can be synthesised at 1200 °C under ambient pressure, this has limiting composition 5H-$BaCrO_{2.8}$ with a fully ordered structure containing double tetrahedral Cr^{4+} layers due to reconstruction of the oxygen-deficient layer. 5H-$BaCrO_{2.8}$ orders antiferromagnetically below 260 K and the magnetic structure has a (0 0 1/2) propogation vector with moments modulated according to the order of Cr^{3+} and Cr^{4+} states.

Acknowledgements

We thank EPSRC and the Royal Society for support, STFC for the provision of beamtime, and Drs. Claire Murray (Diamond) and Ivan da Silva (ISIS) for assistance during data collection.

Open data for this article are at (link to be added at proof stage)

Keywords; reduced oxides · perovskites · high pressure synthesis · vacancy-ordering · magnetic structure

1 Cowin, P. I.; Petit, Ch. T.G.; Lan, R.; Irvine, J.T.S.; Tao, Sh. *Adv. Energy Mater.* 2011, 1, 314-332.

2 Krockenberger, Y., Mogare, K., Reehuis, M., Tovar, M., Jansen, M., Vaitheeswaran, G., Kanchana, V., Bultmark, F., Delin, A., Wilhelm, F., Rogalev, A., Winkler, A. & Alff, L. *Phys. Rev. B* **75**, 020404 (2007).

3 A. J. Williams, A. Gillies, J. P. Attfield**,** G. Heymann, H. Huppertz, M. J. Martínez-Lopez, J. A. Alonso, *Phys. Rev. B.* **2006**, *73*, 104409.

4 J. A. Rodgers, A. J. Williams, A. J. Martinez-Lope, J. A. Alonso and J. P. Attfield. *Chem. Mater.* 20, 4797 – 4799 (2008).

5 L. Ortega-San-Martin, A. J. Williams, J. Rodgers, J. P. Attfield, G. Heymann, J. Huppertz, *Phys. Rev. Lett.* **2007**, *99*, 255701.

6 A. M. Arévalo-López, J. A. Rodgers, M. S. Senn, F. Sher, J. Farnham, W. Gibbs, J. P. Attfield, *Angew. Chem. Int. Ed.* **2012**, *51*, 10791.

7 A. M. Arevalo-Lopez, F. Sher, J. Farnham, A. J. Watson and J. P. Attfield, *Chem. Mater.*, 2013, **25**, 2346.

8 K. H. L. Zhang, P. V. Sushko, R. Colby, Y. Du, M. E. Bowden and S. A. Chambers, *Nat. Comm.* **2014**, 5, 4669.

9 A. M. Arevalo-Lopez, B. Liang, M. S. Senn, C. Murray, C. Tang and J. P. Attfield, *J Mater. Chem. C*, **2014**, 2, 9364.

10 A. M. Arevalo-Lopez and J. P. Attfield, *Dalton Trans.* **2015**, 44, 10661.

11 B. L. Chamberland, *Inorg. Chem* **1969**, *8*, 286.

12 P. S. Haradem, B. L. Chamberland, L. Katz, *J. Solid State Chem.* **1980**, *34*, 59.

13 B. L. Chamberland, *J. Solid State Chem.* **1982**, *43*, 309.

14 B. L. Chamberland, L. Katz, *Acta Cryst.* **1982**, *B38*, 54.

15 B. L. Chamberland, *J. Solid State Chem.* **1983**, *48*, 318.

16 Y. Torii, *Chem. Lett.*, 1975, 557

17 Z. H. Zhu, F. J. Rueckert, J. I. Budnick, W. A. Hines, M. Jain, H. Zhang, and B. O. Wells. *Phys.*

Rev. B, **87**, 195129 (2013).

18 A. M. Arevalo-Lopez, S. J. Reeves, J. P. Attfield *Z. Anorg. Allg. Chem.* **2014**, 640, 2727.

19 O. Mentre, M. Iorgulescu, M. Huve, H. Kabbour, N. Renaut, S. Daviero-Minaud,S. Colis, P. Roussel, *Dalton Trans.* **2015**, 44, 10728.

20 B. L. Chamberland, *J. Solid State Chem.* 1971, 3, 243

21 K. Nishimura, I. Yamada, K. Oka, Y. Shimakawa, M. Azuma, *J Phys Chem Sol* 2014, 75, 710

22 G. Liu and J. E. Greedan, *J. Solid State Chem.* **1994**, 110, 274

23 Boulahya, K.; Parras, M.; Gonzalez-Calbet, J. M.; Amador, U.; Martinez, J. L.; Tissen, V.; Fernandez-Diaz, M. T. *Phys. Rev. B* **2005**, 71, 144402.

24 N. E. Brese, M. O'Keeffe, *Acta Cryst. B* **1991**, *47*, 192-197.

25 J. P. Attfield, *Solid State Sci.* 8, 861 (2006).

26 A.J. Jacobson, J.L. Hutchison, *J. Solid State Chem.* 1980, 35, 334.

27 Haag, J. M.; Madsen, B. D.; Barnett, S. A.; Poeppelmeier, K. R. *Electrochem. Solid-State Lett.* 2008, 11, B51.

Table of Contents

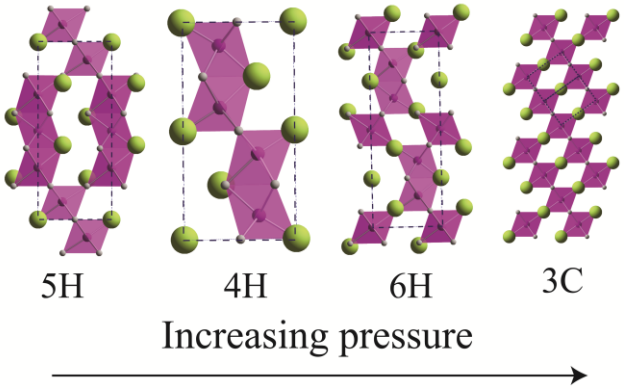

Hexagonal 5H, 4H, and 6H perovskites polytypes of $BaCrO_3$ are observed with increasing pressure and the cubic 3C perovskite is stabilised in bulk form for the first time at 19-22 GPa. Oxygen-deficient 5H-$BaCrO_{2.8}$ synthesised at ambient pressure contains double tetrahedral Cr^{4+} layers and orders antiferromagnetically below 260 K with a (0 0 1/2) magnetic structure.